

Effects of next-to-leading order DGLAP evolution on generalized parton distributions of the proton and deeply virtual Compton scattering at high energy

Hamzeh Khanpour^{1,2,*}, Muhammad Goharipour^{3,†} and Vadim Guzey^{4‡}

⁽¹⁾Department of Physics, University of Science and Technology of Mazandaran, P.O.Box 48518-78195, Behshahr, Iran

⁽²⁾School of Particles and Accelerators, Institute for Research in Fundamental Sciences (IPM), P.O.Box 19395-5531, Tehran, Iran

⁽³⁾Department of Physics, Aliabad katoul Branch, Islamic Azad University, Aliabad katoul, Iran

⁽⁴⁾National Research Center “Kurchatov Institute”, Petersburg Nuclear Physics Institute (PNPI), Gatchina, 188300, Russia

(Dated: August 22, 2017)

We studied the effects of NLO Q^2 evolution of generalized parton distributions (GPDs) using the aligned-jet model for the singlet quark and gluon GPDs at an initial evolution scale. We found that the skewness ratio for quarks is a slow logarithmic function of Q^2 reaching $r^S = 1.5 - 2$ at $Q^2 = 100$ GeV² and $r^g \approx 1$ for gluons in a wide range of Q^2 . Using the resulting GPDs, we calculated the DVCS cross section on the proton in NLO pQCD and found that this model in conjunction with modern parameterizations of proton PDFs (CJ15 and CT14) provides a good description of the available H1 and ZEUS data.

I. INTRODUCTION

Generalized parton distributions (GPDs) have become a familiar and standard tool of Quantum Chromodynamics (QCD) describing the response of hadronic targets in various hard exclusive processes [1–8]. GPDs can be rigorously defined in the framework of QCD collinear factorization for hard exclusive processes [9, 10], which allows one to access universal, i.e., process-independent, GPDs in such processes as deeply virtual Compton scattering (DVCS) $\gamma^* + T \rightarrow \gamma + T$, timelike Compton scattering (TCS) $\gamma + T \rightarrow \gamma^* + T$, exclusive meson production by longitudinally polarized photons $\gamma_L^* + T \rightarrow M + T$, and, recently, photoproduction of heavy (J/ψ , Υ) vector mesons $\gamma + T \rightarrow V + T$ [11, 12]. GPDs contain information on the hadron structure in QCD, which is hybrid of that encoded in usual parton distributions and elastic form factors. In particular, GPDs describe the distributions of quarks and gluons in hadrons in terms of two light-cone momentum fractions and the position in the transverse plane. Also, GPDs are involved in the hadron spin decomposition in terms of the helicity and orbital motion contributions of quarks and gluons [4–8], and carry information on the spatial distribution of forces experienced by partons inside hadrons [13].

GPDs are essentially non-perturbative quantities, which cannot be calculated from the first principles apart from first Mellin moments in special cases in lattice QCD [14, 15]. At the same time, evolution of GPDs with an increase of the resolution scale Q^2 is predicted by the QCD Dokshitzer–Gribov–Lipatov–Altarelli–Parisi (DGLAP) evolution equations modified to the case of GPDs, which are presently known to the next-to-leading

order (NLO) accuracy [16–18]. Therefore, one of directions of phenomenological studies of GPDs is to determine the non-perturbative input for these evolution equations. After early studies of GPDs using various dynamical models of the nucleon structure [19–26], one currently focuses on parameterizations of GPDs, which are determined from fitting the available data. The two main contemporary approaches include the flexible parameterization based on the conformal expansion of GPDs [27–30] and global fits of GPDs [31–34], which use the double distribution (DD) model [35–39] in the Vanderhaeghen–Guichon–Guidal (VGG) framework, see details in [33]. One should also mention a pioneering study of global QCD fits of GPDs within the neural network approach [40].

The mentioned above analyses present only a partial, model-dependent picture of GPDs in a limited kinematic range. For further progress, it is important to perform a systematic QCD analysis of evolution of GPDs and cross sections of hard exclusive processes involving them. It will enable one to separate the effects of non-perturbative input GPDs from the perturbative DGLAP evolution and help to explore the possibility to use the data on hard exclusive reactions at high energies for constraining GPDs, see, e.g. [41].

In this paper, we calculate the effect of next-to-leading (NLO) QCD evolution on quark and gluon GPDs of the proton using the brute-force evolution method of [16–18] and the physical model for input GPDs, which is motivated by the the aligned-jet model [26]. Using the obtained results, we calculate the DVCS cross section on the proton in NLO QCD and compare it to the available HERA data. We find that our approach provides a good description of the data.

* Hamzeh.Khanpour@mail.ipm.ir

† Muhammad.Goharipour@gmail.com

‡ guzey_va@pnpi.nrcki.ru

II. ALIGNED-JET MODEL FOR GPDs AND QCD EVOLUTION EFFECTS

A. Input GPDs

The aligned-jet model (AJM) [42, 43] for photon–hadron interactions at high energies is based on the general observation that in the target rest frame, the incoming photon first fluctuates into quark-antiquark configurations, which then interact with the target. For the photon virtualities $Q^2 = \mathcal{O}(\text{few}) \text{ GeV}^2$, the $q\bar{q}$ pair (dipole) is characterized by a small relative transverse momentum (hence the name aligned-jet), the invariant mass of the order of Q^2 , the asymmetric sharing of the photon's light-cone momentum, and the dipole–nucleon cross section, which has the magnitude typical for hadron–nucleon cross sections. Note that in QCD, this parton picture is complimented by the gluon emission and the contribution of quark-antiquark dipoles with large relative transverse momenta, which become progressively important as Q^2 is increased; see the discussion in Ref. [44]. In the AJM model, one obtains for the ratio of the imaginary parts of DVCS and DIS amplitudes at $Q^2 = 1 - 3 \text{ GeV}^2$, $R = \mathcal{Im} \mathcal{T}_{\text{DVCS}} / \mathcal{Im} \mathcal{T}_{\text{DIS}} = 2.5 - 3.5$ [26, 45], which agrees nicely with the values of R extracted from the HERA data [46]. This in turn means that the effect of skewness of the singlet quark GPDs in the DGLAP region of $X \geq \zeta$ can be neglected (X is the light-cone momentum fraction of the target in the initial state carried by the interacting parton; ζ is the momentum fraction difference between the two interacting partons). This observation is also supported by the analysis of Ref. [6], which showed that the good description of the high-energy HERA data on the DVCS cross section on the proton can be achieved with the forward parton distribution model for the singlet quark GPDs [47, 48], i.e., with the δ -function-like profile in the DD model for sea quark GPDs.

Starting from a model for GPDs in the DGLAP region of $X \geq \zeta$, there is no unique and simple way to reconstruct GPDs in the entire range of X . For instance, the method proposed in [26, 46] does not guarantee polynomiality for higher moments of GPDs and conflicts with dispersion relations (DR) for the real and imaginary parts of the DVCS amplitude [49]. In principle, GPDs with the correct forward limit and satisfying the property of polynomiality can be constructed using the so-called Shuvaev transform [50–52]. However, this method is usually associated with the leading order (LO) phenomenology and also brings certain skewness dependence of GPDs in the DGLAP region. Similarly, the flexible parameterization of GPDs based on the conformal expansion [27–30] contains the skewness effect of GPDs in the DGLAP region and also corresponds to model-dependent parton distributions in the forward limit.

In this work, to simultaneously have the forward-like GPDs in the DGLAP region and circumvent the aforementioned problem with polynomiality, we take forward-like GPDs for all X and add the so-called D -term [53],

which has support only in the Efremov–Raduyshkin–Brodsky–Lepage (ERBL) region of $|X| \leq \zeta$. Specifically, we use the following model for the singlet quark (one sums over quark flavors q) and gluon GPDs at $t = 0$ at the initial scale of μ_0 :

$$(1 - \zeta/2)H^S(X, \zeta, t = 0, \mu_0) = \begin{cases} \sum_q [q(x, \mu_0) + \bar{q}(x, \mu_0)] + D^S(x/\eta) \theta(\zeta - X), & X > \zeta/2 \\ -\sum_q [q(x, \mu_0) + \bar{q}(x, \mu_0)] - D^S(x/\eta) \theta(\zeta - X), & X < \zeta/2 \end{cases} \\ (1 - \zeta/2)H^g(X, \zeta, t = 0, \mu_0) = |x|g(|x|, \mu_0), \quad (1)$$

where $x = (X - \zeta/2)/(1 - \zeta/2)$ and $\eta = \zeta/(2 - \zeta)$; $q(x, \mu)$ and $g(x, \mu)$ are the quark and gluon parton distribution functions (PDFs), respectively. Note that since we explicitly introduced antiquark GPDs, it is sufficient to consider only non-negative $X \geq 0$. As follows from general properties of GPDs, the singlet quark GPD $H^S(X, \zeta, t = 0, \mu_0)$ is antisymmetric in the ERBL region around the $X = \zeta/2$ point, while the gluon GPD $H^g(X, \zeta, t = 0, \mu_0)$ is symmetric in the ERBL region.

The function $D^S(x/\eta)$ is the singlet quark D -term [53], which can be expanded in terms of odd Gegenbauer polynomials $C_n^{3/2}$ in the following form [54]:

$$D^S(z, \mu_0) = 2(1 - z^2)[d_1 C_1^{3/2}(z) + d_3 C_3^{3/2}(z) + d_5 C_5^{3/2}(z)]. \quad (2)$$

The coefficients d_1 , d_3 and d_5 were estimated in the chiral quark soliton model at $\mu_0 = 0.6 \text{ GeV}$ in Ref. [20]: $d_1 = -4$, $d_3 = -1.2$, and $d_5 = -0.4$. Note that due to the lack of numerical estimates, we neglected the possible gluon D -term in Eq. (1). In this case, $D^S(z, \mu)$ evolves in μ^2 autonomously (without mixing) and its value for $\mu > \mu_0$ can be readily calculated.

By construction, see Eq. (1), in the middle of the ERBL region at $x = X - \zeta/2 = 0$, our singlet quark GPDs become singular and the gluon GPD vanishes. Being a natural artifact of our model imposing the correct GPD symmetry in the ERBL problem, it does not violate general principles of GPDs and does not conflict with factorization for amplitudes of hard exclusive processes. Since the main goal of our work is to study the effects of NLO Q^2 evolution of GPDs in conjunction with different baseline PDFs, the simple model of Eq. (1) should suffice.

Note that in this work, we consider only the singlet $q + \bar{q}$ and gluon GPDs: valence quark GPDs do not mix with singlet quark and gluon GPDs under the DGLAP evolution and do not separately contribute to the DVCS amplitude.

B. NLO Q^2 evolution of GPDs

The determination of parton distribution functions (PDFs) has always been one of the important ingredients for theory predictions. In this respect, more accurate PDFs play an important role in understanding of hadronic properties and the structure of the nucleon [55–58]. From past to present, our knowledge of PDFs has

been developed both theoretically and computationally. However, results of various groups lead to different predictions of physical observables. As we know, generalized PDFs (GPDs) are quantities that are related to the PDFs in the forward limit and in many phenomenological approaches. To investigate the impact of different PDFs on the GPDs and their evolution, we calculate the effect of next-to-leading order (NLO) DGLAP evolution equations modified to the case of GPDs using the formalism of [16–18] and the input GPDs of Eqs. (1). (The early results on leading order (LO) Q^2 evolution of GPDs were presented in Refs. [50, 59].) For the forward PDFs, we used CT14 [60] and the new CTEQ-Jefferson Lab (CJ15) analysis [61]. To study the impact of PDF uncertainties on the GPD evolutions and DVCS cross sections, we include the uncertainties of CT14 and CJ15 PDFs in the calculations of the evolution and also in the DVCS cross sections.

Figures 1 and 2 show the results for the singlet quark GPD $H^S(X, \zeta, t = 0, Q^2)$ and the gluon GPD $H^g(X, \zeta, t = 0, Q^2)$, respectively, as a function of X at $\zeta = 0.001$ and $Q^2 = 1.69, 4, 10$, and 100 GeV^2 . Note that $Q^2 = 1.69 \text{ GeV}^2$ is the input scale for CT14 and CJ15. As can be seen from these figures, the Q^2 evolution pushes GPDs into the ERBL region of $X < \zeta$ as it should be. In the singlet quark case, the difference between the predictions based on CT14 and CJ15 PDF is small, especially at lower values of the Q^2 resolution scale. At the same time, in the gluon channel the differences between the CT14 and CJ15 predictions are sizable and exceed the associated uncertainties for large values of Q^2 . One should also note that the uncertainties of the resulting GPDs based on CT14 are larger than those for CJ15, which is related to the large uncertainties of CT14 singlet distributions at small x . Generally speaking, our results indicate that the GPD model of Eq. (1) is sensitive to input PDFs. Therefore, more accurate PDFs are very important for physical observables involving GPDs such as, e.g., DVCS cross sections. Conversely and optimistically, data on the DVCS cross section may provide new constraints for global QCD analysis of PDFs.

C. Effect of skewness

To quantify the effect of skewness, it is convenient to introduce the following ratios of quark and gluon GPDs and PDFs [28]:

$$\begin{aligned} r^S(\zeta, \mu) &= \frac{(1 - \zeta/2)H^S(\zeta, \zeta, t = 0, \mu)}{\sum_q [q(\zeta/(2 - \zeta), \mu) + \bar{q}(\zeta/(2 - \zeta), \mu)]}, \\ r^g(\zeta, \mu) &= \frac{(1 - \zeta/2)H^g(\zeta, \zeta, t = 0, \mu)}{\zeta/(2 - \zeta)g(\zeta/(2 - \zeta), \mu)}. \end{aligned} \quad (3)$$

Our results for $r^S(\zeta, \mu)$ and $r^g(\zeta, \mu)$ as functions $Q^2 = \mu^2$ at $\zeta = 0.001$ are shown in Fig. 3. One can see from the figure that both r^S and r^g are slow logarithmic functions of Q^2 . By construction, $r^S = r^g = 1$ at the initial evo-

lution scale of $Q^2 = 1.69 \text{ GeV}^2$. As Q^2 is increased, r^S slowly increases up to $r^S \approx 1.5 - 2$ at $Q^2 = 100 \text{ GeV}^2$, while r^g stays at the level of unity for the studied range of Q^2 .

These results agree with the predictions of the flexible GPD parameterization based on the conformal expansion, see Fig. 7 of Ref. [28], except for r^S at the input $Q^2 = 1.69 \text{ GeV}^2$, where our result lies lower than that of [28].

III. DEEPLY VIRTUAL COMPTON SCATTERING AT HERA

Using our model for the singlet quark and gluon GPDs of the proton, we make predictions for the DVCS cross section in NLO perturbative QCD. Our results are presented in Figs. 4, 5, 6, 7, 8 and 9, where they are compared to the available HERA data of the H1 [62, 64, 65, 67] and ZEUS [63, 66] measurements (see Table I). The error bars the statistical and systematic uncertainties added in quadrature. The bands associated with CJ15 and CT14 prediction correspond to the uncertainty on the respective PDFs.

It is worth mentioning that we assume an exponential and factorized t -dependence of the DVCS cross section, $e^{-b(Q^2)|t|}$. The Q^2 dependence of the t -slope parameter $b(Q^2)$ is introduced using the following formula $b(Q^2) = a[1 - c \ln(Q^2/2 \text{ GeV}^2)]$, with $a = 8 \text{ GeV}^{-2}$ and $c = 0.15$ [26].

One can see from these figures that within experimental and theoretical uncertainties, the input GPD model based on the CJ15 fit provides a good description of the H1-2001, H1-2005, H1-2007 and H1-2009 data (Q^2 dependence only for the two latter data sets), while the model based on the CT14 fit tends to somewhat overestimate the cross section normalization (it describes well the W dependence of the H1-2005, H1-2007 and H1-2009 data). At the same time, the CT14 parametrization leads to a very good description of the ZEUS data. These results clearly show that for some selected PDF sets, such as, e.g., the CJ15 and CT14 fits, the AJM GPD model of [26] together with NLO pQCD calculations can describe well the high-energy DVCS cross section. Consequently one can use these sets of PDFs for future fitting procedures.

In order to study effects of the NLO DGLAP evolution on GPDs, a detailed comparison of our obtained results with the DVCS $\gamma^* p \rightarrow \gamma p$ cross section is shown in Fig. 10. The comparison has been shown as a function of W for some selected values of $Q^2 = 2.4, 6.2, 9.9$ and 18 GeV^2 . The NLO pQCD predictions are based on our input of Eq. (1) and CT14 [60] PDFs. The results are compared to the 2003 and 2008 ZEUS data [63, 66]. The inner error bars represent the statistical, and the full error bars the quadratic sum of the statistical and systematic uncertainties. One can see that a very good agreement between our predictions and ZEUS data is achieved for a wide range of Q^2 and W .

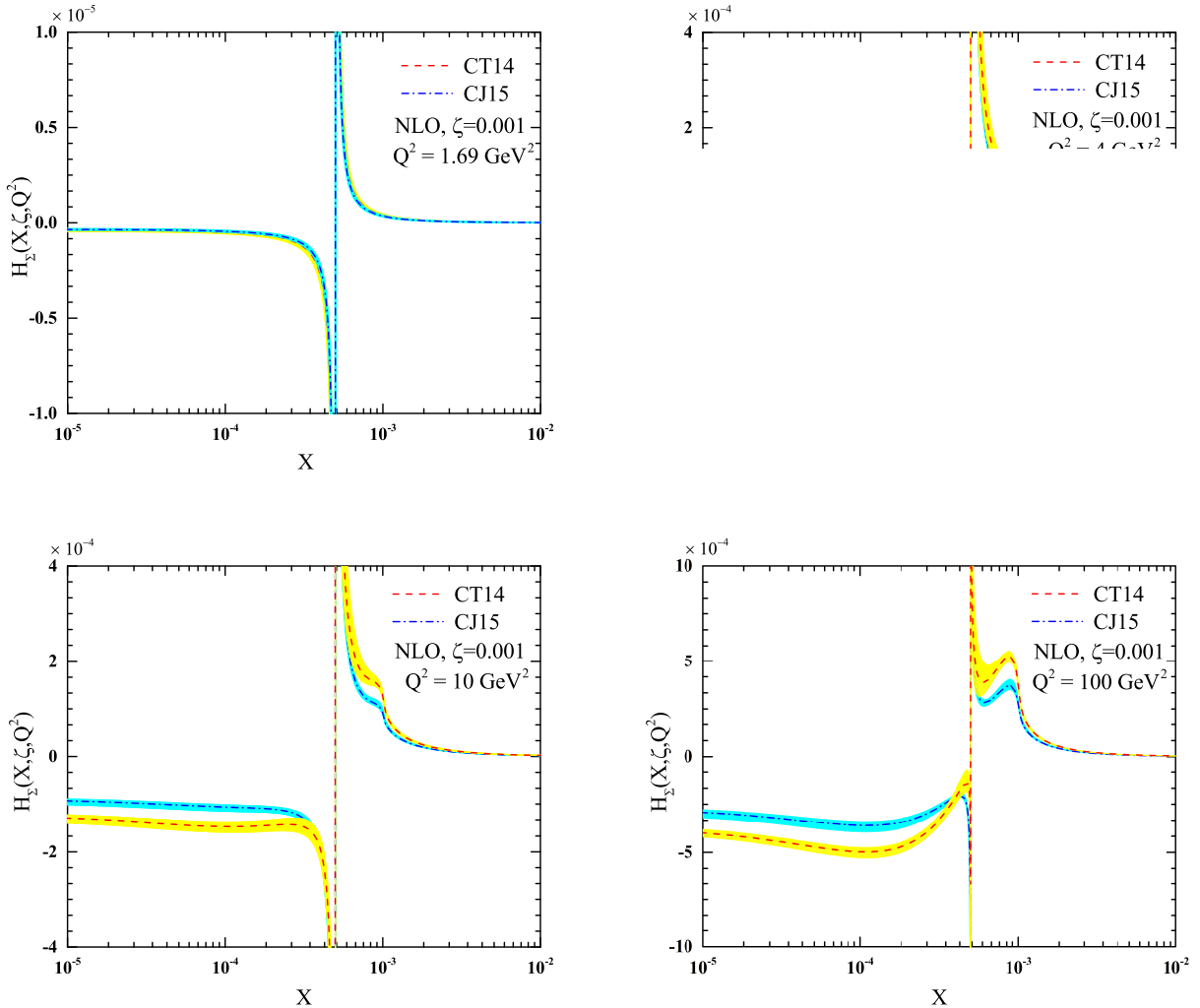


Figure 1: (Color online) The singlet quark GPD $H^S(X, \zeta, t = 0, Q^2)$ as a function of X at $\zeta = 0.001$ and $Q^2 = 1.69, 4, 10$ and 100 GeV^2 . The GPDs are calculated using the input of Eq. (1) with the CT14 [60] and CJ15 [61] parameterizations of PDFs and NLO Q^2 evolution for GPDs.

Collaboration	Observables	$Q^2 [\text{GeV}^2]$	$W [\text{GeV}]$	Year	Reference
H1	$\sigma_{\text{DVCS}}(Q^2), \sigma_{\text{DVCS}}(W)$	2-20	30-120	2001	[62]
H1	$\sigma_{\text{DVCS}}(Q^2), \sigma_{\text{DVCS}}(W)$	2-80	30-140	2005	[64]
H1	$\sigma_{\text{DVCS}}(Q^2), \sigma_{\text{DVCS}}(W), \sigma_{\text{DVCS}}(Q^2, W)$	6.5-80	30-140	2007	[65]
H1	$\sigma_{\text{DVCS}}(Q^2), \sigma_{\text{DVCS}}(W), \sigma_{\text{DVCS}}(Q^2, W)$	6.5-80	30-140	2009	[67]
ZEUS	$\sigma_{\text{DVCS}}(Q^2), \sigma_{\text{DVCS}}(W), \sigma_{\text{DVCS}}(Q^2, W)$	5-100	40-140	2003	[63]
ZEUS	$\sigma_{\text{DVCS}}(Q^2), \sigma_{\text{DVCS}}(W), \sigma_{\text{DVCS}}(Q^2, W)$	1.5-100	40-170	2008	[66]

Table I: Overview of DVCS on proton experiments at HERA collider used in this study. The observable σ_{DVCS} is the cross section for the sub-process $\gamma^* p \rightarrow \gamma p$.

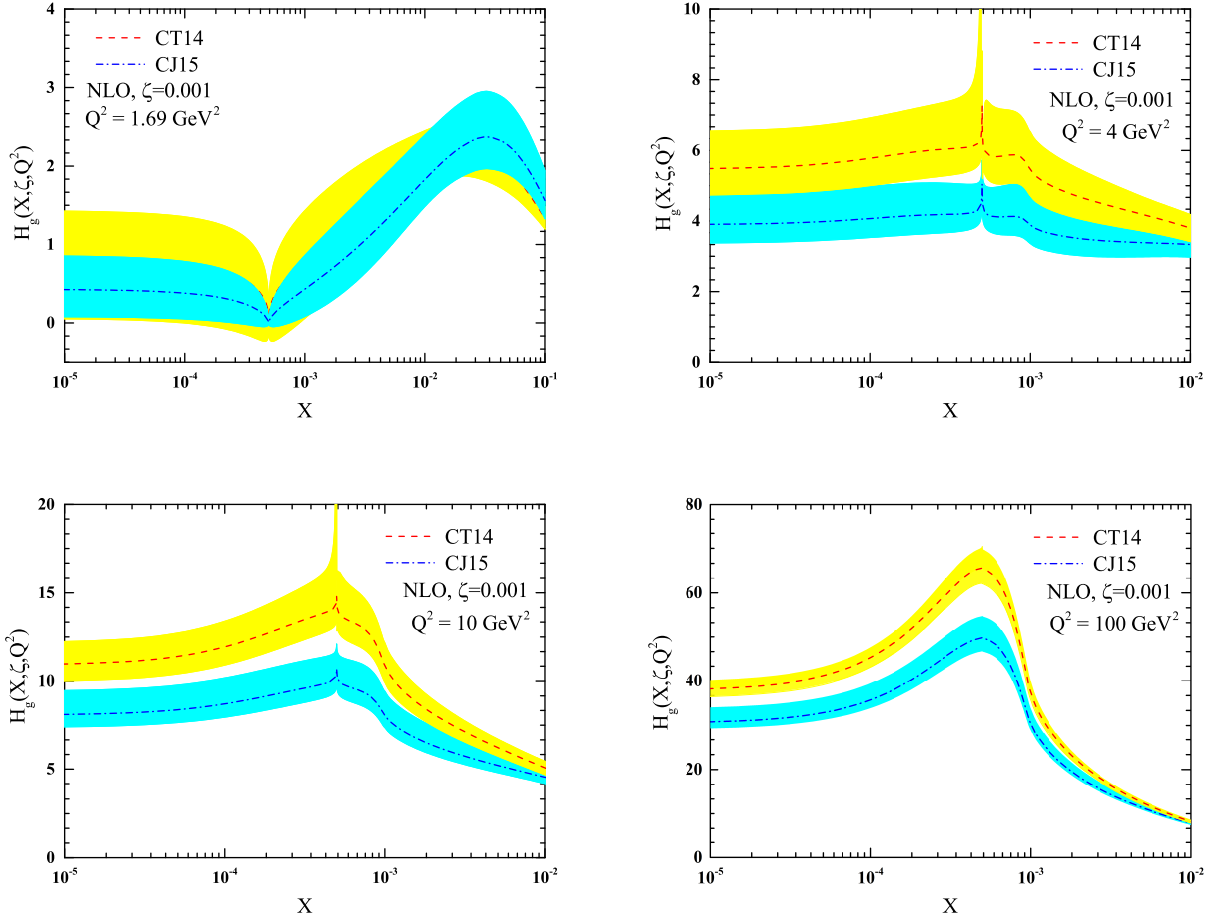


Figure 2: (Color online) The gluon GPD $H^g(X, \zeta, t = 0, Q^2)$ as a function of X at $\zeta = 0.001$ and $Q^2 = 1.69, 4, 10$ and 100 GeV^2 . See Fig. 1 for details.

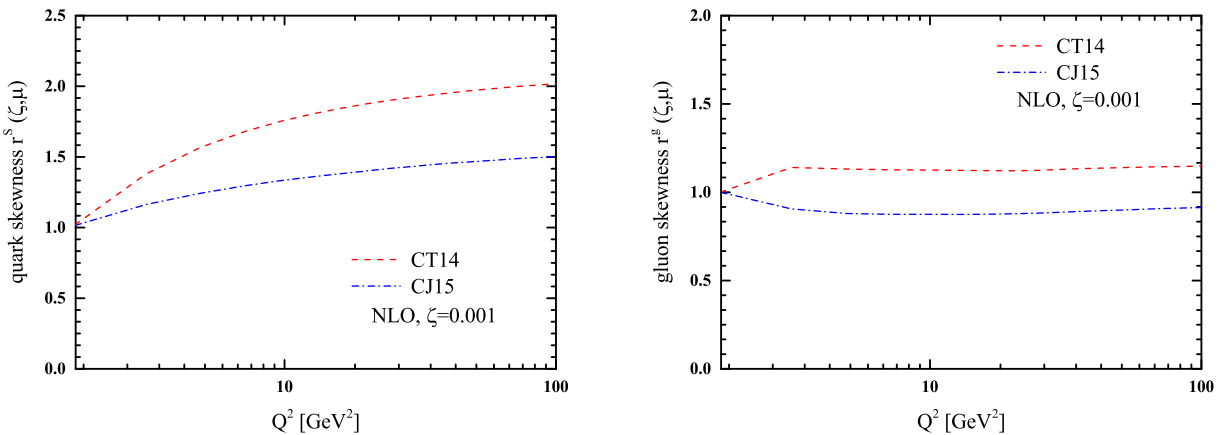


Figure 3: (Color online) The quark and gluon skewness ratios $r^S(\zeta, \mu)$ (left) and $r^g(\zeta, \mu)$ (right) as functions $Q^2 = \mu^2$ at $\zeta = 0.001$.

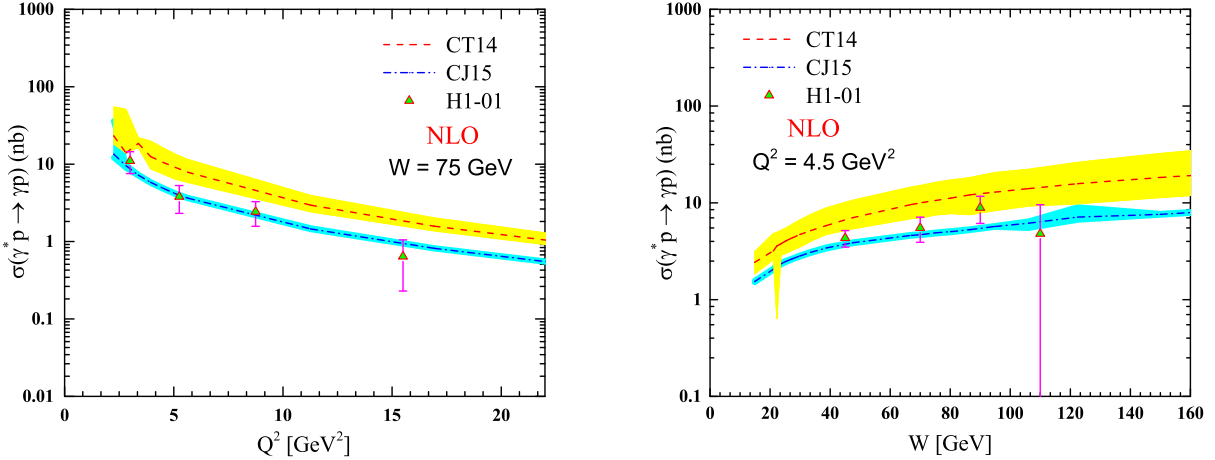


Figure 4: (Color online) The DVCS $\gamma^* p \rightarrow \gamma p$ cross section as a function of Q^2 (left) and W (right). The 2001 H1 data [62], where the statistical and systematical errors are added in quadrature, is compared to our NLO pQCD results based on the input of Eq. (1) and CT14 [60] and CJ15 [61] PDFs. The shadowed bands represent the uncertainty of the corresponding PDFs.

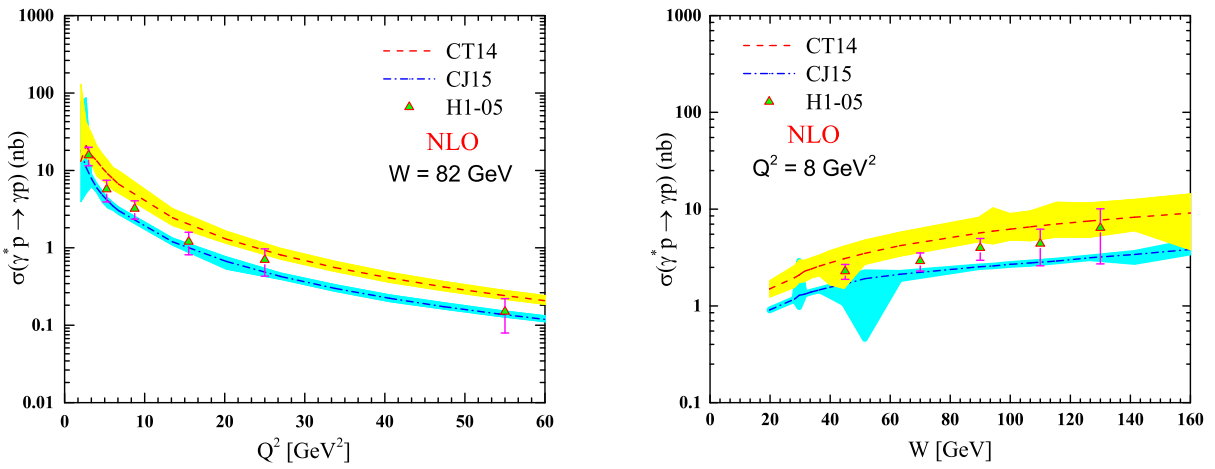


Figure 5: (Color online) The DVCS $\gamma^* p \rightarrow \gamma p$ cross section as a function of Q^2 (left) and W (right). Our NLO pQCD results are compared to the 2005 H1 data [64], see details in Fig. 4.

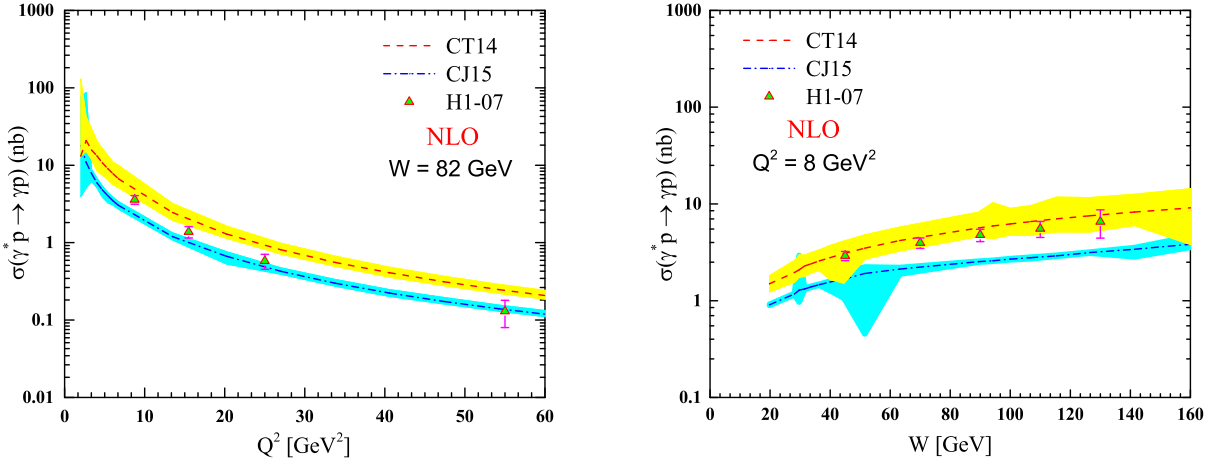


Figure 6: (Color online) The DVCS $\gamma^* p \rightarrow \gamma p$ cross section as a function of Q^2 (left) and W (right). Our NLO pQCD results are compared to the 2007 H1 data [65], see details in Fig. 4.

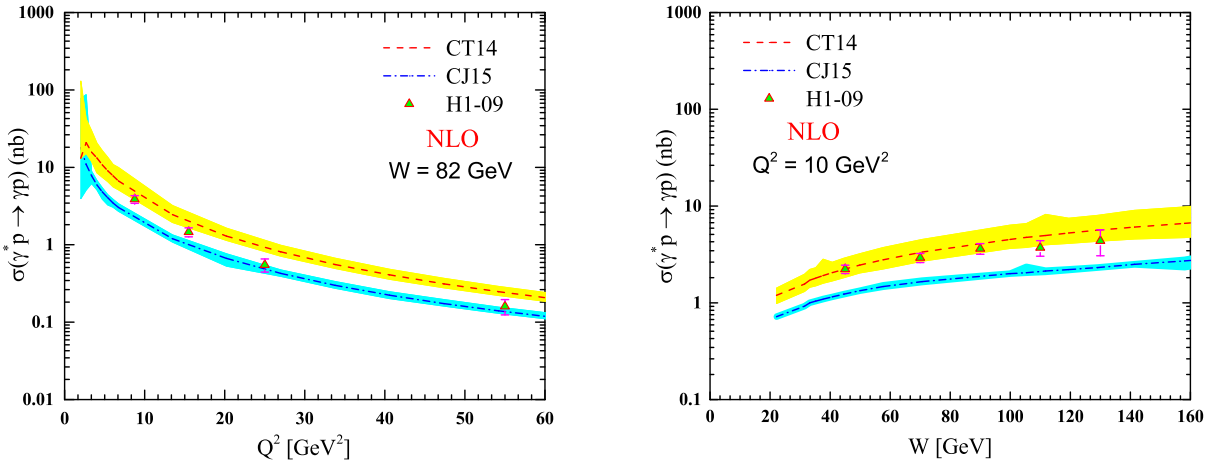


Figure 7: (Color online) The DVCS $\gamma^* p \rightarrow \gamma p$ cross section as a function of Q^2 (left) and W (right). Our NLO pQCD results are compared to the 2009 H1 data [67], see details in Fig. 4.

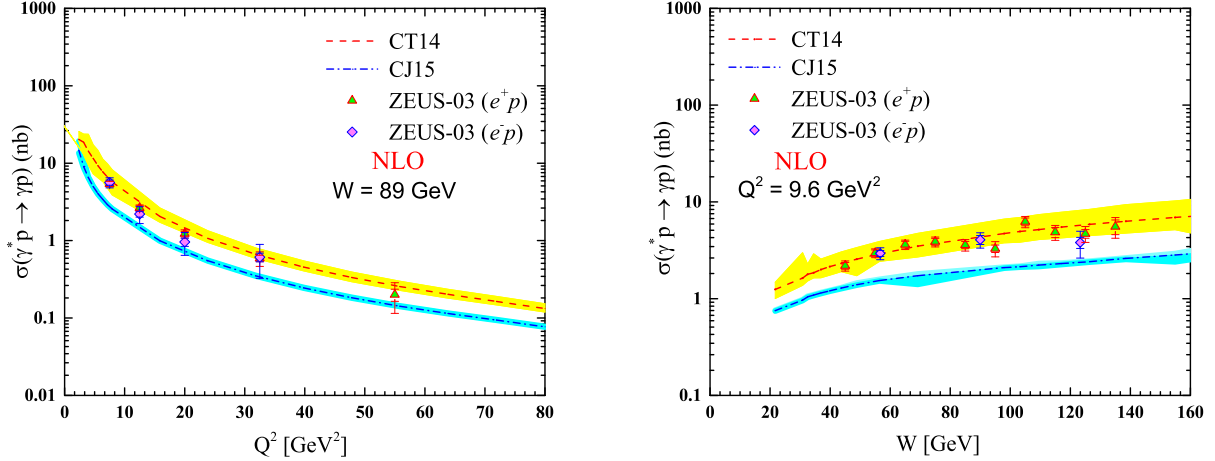


Figure 8: (Color online) The DVCS $\gamma^* p \rightarrow \gamma p$ cross section as a function of Q^2 (left) and W (right). Our NLO pQCD results are compared to the 2003 ZEUS data [63], see details in Fig. 4. The inner error bars represent the statistical errors, and the outer error bars the statistical and systematic errors added in quadrature.

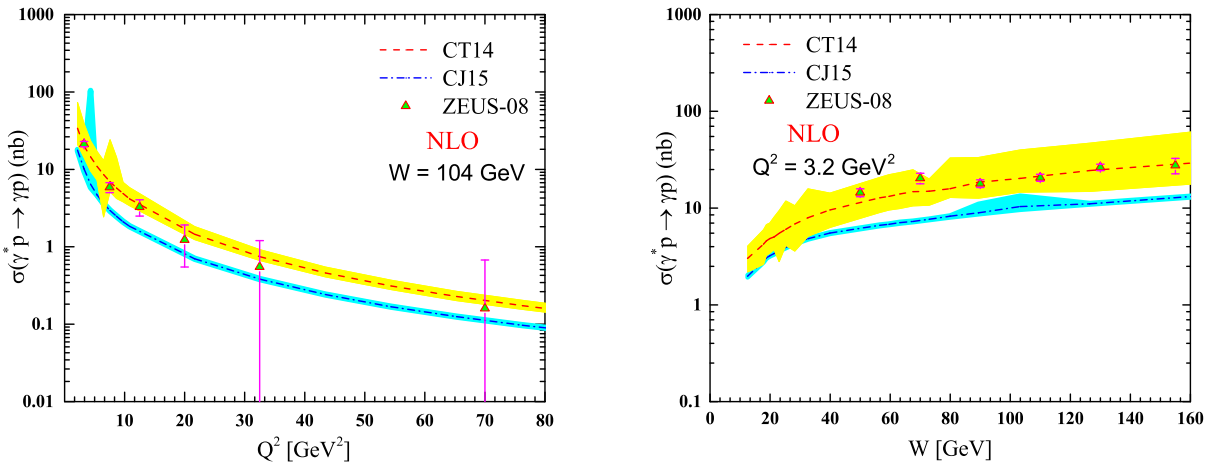


Figure 9: (Color online) The DVCS $\gamma^* p \rightarrow \gamma p$ cross section as a function of Q^2 (left) and W (right). Our NLO pQCD results are compared to the 2008 ZEUS data [66], see details in Fig. 4.

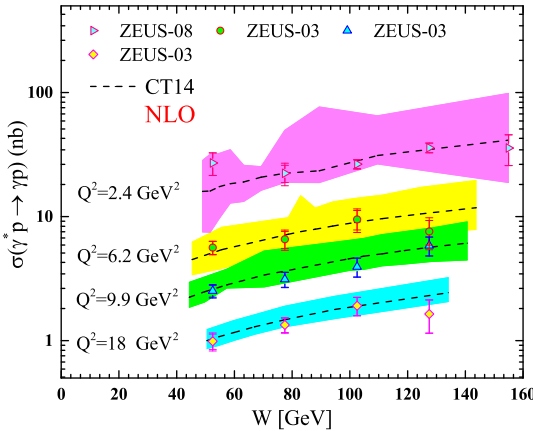


Figure 10: (Color online) The DVCS $\gamma^* p \rightarrow \gamma p$ cross section as a function of W for some selected values of $Q^2 = 2.4, 6.2, 9.9$ and 18 GeV^2 . The NLO pQCD predictions are based on the input of Eq. (1) and CT14 [60]. The results are compared to the 2003 and 2008 ZEUS data [63, 66].

IV. CONCLUSIONS

In this work, we studied the effects of NLO Q^2 evolution of GPDs using a model for the singlet quark and gluon GPDs at an initial evolution scale motivated by the aligned-jet model of photon–hadron interactions at high energies. Quantifying the evolution effects by the GPD-to-PDF ratios r^S and r^g , we found that r^S increases logarithmically slowly from $r^S = 1$ at the input scale of $Q^2 = 1.69 \text{ GeV}^2$ to $r^S = 1.5–2$ at $Q^2 = 100 \text{ GeV}^2$; in the gluon channel, $r^g \approx 1$ for the studied range of Q^2 . This observation agrees with the results of the more sophisticated model of GPDs based on conformal expansion [28].

Using the resulting GPDs, we calculated the DVCS cross section on the proton in NLO pQCD and compared it to the available HERA data. We found that our simple physical model of input GPDs used in conjunction with two modern parameterizations of proton PDFs (CJ15 and CT14) provides good description of the H1 and ZEUS data.

ACKNOWLEDGMENTS

VG would like to thank M. Strikman and M. Diehl for useful discussions of the model of input GPDs used in this analysis. HK acknowledges the University of Science and Technology of Mazandaran and School of Particles and Accelerators, Institute for Research in Fundamental Sciences (IPM) for financial support provided for this research.

-
- [1] D. Müller, D. Robaschik, B. Geyer, F.-M. Dittes and J. Hořejši, *Fortsch. Phys.* **42**, 101 (1994) doi:10.1002/prop.2190420202 [hep-ph/9812448].
- [2] A. V. Radyushkin, *Phys. Rev. D* **56**, 5524 (1997) doi:10.1103/PhysRevD.56.5524 [hep-ph/9704207].
- [3] X. D. Ji, *Phys. Rev. D* **55**, 7114 (1997) doi:10.1103/PhysRevD.55.7114 [hep-ph/9609381].
- [4] X. D. Ji, *J. Phys. G* **24**, 1181 (1998) doi:10.1088/0954-3899/24/7/002 [hep-ph/9807358].
- [5] K. Goeke, M. V. Polyakov and M. Vanderhaeghen, *Prog. Part. Nucl. Phys.* **47**, 401 (2001) doi:10.1016/S0146-6410(01)00158-2 [hep-ph/0106012].
- [6] A. V. Belitsky, D. Mueller and A. Kirchner, *Nucl. Phys. B* **629**, 323 (2002) doi:10.1016/S0550-3213(02)00144-X [hep-ph/0112108].
- [7] M. Diehl, *Phys. Rept.* **388**, 41 (2003) doi:10.1016/j.physrep.2003.08.002, 10.3204/DESY-THESIS-2003-018 [hep-ph/0307382].
- [8] A. V. Belitsky and A. V. Radyushkin, *Phys. Rept.* **418**, 1 (2005) doi:10.1016/j.physrep.2005.06.002 [hep-ph/0504030].
- [9] J. C. Collins and A. Freund, *Phys. Rev. D* **59**, 074009 (1999) doi:10.1103/PhysRevD.59.074009 [hep-ph/9801262].
- [10] J. C. Collins, L. Frankfurt and M. Strikman, *Phys. Rev. D* **56**, 2982 (1997) doi:10.1103/PhysRevD.56.2982 [hep-ph/9611433].
- [11] D. Y. Ivanov, A. Schafer, L. Szymanowski and G. Krasnikov, *Eur. Phys. J. C* **34**, no. 3, 297 (2004) Erratum: [*Eur. Phys. J. C* **75**, no. 2, 75 (2015)] doi:10.1140/epjc/s2004-01712-x, 10.1140/epjc/s10052-015-3298-8 [hep-ph/0401131].
- [12] S. P. Jones, A. D. Martin, M. G. Ryskin and T. Teubner, *J. Phys. G* **43**, no. 3, 035002 (2016) doi:10.1088/0954-3899/43/3/035002 [arXiv:1507.06942 [hep-ph]].
- [13] M. V. Polyakov, *Phys. Lett. B* **555**, 57 (2003) doi:10.1016/S0370-2693(03)00036-4 [hep-ph/0210165].
- [14] P. Hagler *et al.* [LHPC Collaboration], *Phys. Rev. D* **77**, 094502 (2008) doi:10.1103/PhysRevD.77.094502 [arXiv:0705.4295 [hep-lat]].
- [15] C. Alexandrou, M. Constantinou, S. Dinter, V. Drach, K. Jansen, C. Kallidonis and G. Koutsou, *Phys. Rev. D* **88**, no. 1, 014509 (2013) doi:10.1103/PhysRevD.88.014509 [arXiv:1303.5979 [hep-lat]].
- [16] A. Freund and M. F. McDermott, *Phys. Rev. D* **65**, 091901 (2002) doi:10.1103/PhysRevD.65.091901 [hep-ph/0106124].

- B **429**, 414 (1998)] doi:10.1016/S0370-2693(97)01152-0 [hep-ph/9703449].
- [60] S. Dulat *et al.*, Phys. Rev. D **93**, no. 3, 033006 (2016) doi:10.1103/PhysRevD.93.033006 [arXiv:1506.07443 [hep-ph]].
- [61] A. Accardi, L. T. Brady, W. Melnitchouk, J. F. Owens and N. Sato, Phys. Rev. D **93**, no. 11, 114017 (2016) doi:10.1103/PhysRevD.93.114017 [arXiv:1602.03154 [hep-ph]].
- [62] C. Adloff *et al.* [H1 Collaboration], Phys. Lett. B **517**, 47 (2001) doi:10.1016/S0370-2693(01)00939-X [hep-ex/0107005].
- [63] S. Chekanov *et al.* [ZEUS Collaboration], Phys. Lett. B **573**, 46 (2003) doi:10.1016/j.physletb.2003.08.048 [hep-ex/0305028].
- [64] A. Aktas *et al.* [H1 Collaboration], Eur. Phys. J. C **44**, 1 (2005) doi:10.1140/epjc/s2005-02345-3 [hep-ex/0505061].
- [65] F. D. Aaron *et al.* [H1 Collaboration], Phys. Lett. B **659**, 796 (2008) doi:10.1016/j.physletb.2007.11.093 [arXiv:0709.4114 [hep-ex]].
- [66] S. Chekanov *et al.* [ZEUS Collaboration], JHEP **0905**, 108 (2009) doi:10.1088/1126-6708/2009/05/108 [arXiv:0812.2517 [hep-ex]].
- [67] F. D. Aaron *et al.* [H1 Collaboration], Phys. Lett. B **681**, 391 (2009) doi:10.1016/j.physletb.2009.10.035 [arXiv:0907.5289 [hep-ex]].